

# PHASE MODULATION INDUCED PARTICLE DIFFUSION

M. Ball, J. Budnick, C.M. Chu, M. Ellison, B. Hamilton, D. Jeon,  
X. Kang, L.L. Kiang, S.Y. Lee, A. Pei, A. Riabko, T. Sloan, IUCF, USA  
K.Y. Ng, Fermilab, USA  
M. Syphers, BNL, USA

## Abstract

Experiment measurement of particle diffusion by employing phase modulation to the rf system has been carried out at the IUCF Cooler ring. We measured the evolution of the mountain range, and deduce the rms value of the bunch profile. Our data shows that global chaos plays a dominant role in the particle diffusion mechanism.

## 1 INTRODUCTION

In a space-charge dominated storage ring, the beam intensity is limited because of stability problem. A secondary rf cavity operating at higher harmonic number could increase the beam intensity threshold by flattening the potential well[?]. Thus, the equilibrium beam profile following this flattened potential well would allow a higher ratio of the average current to the peak current. Such a double rf systems have been successfully applied to several low energy synchrotrons[?]. Furthermore, a phase modulation can be applied to one of the rf systems as a *random* noise to perform a controlled particle beam diffusion in the phase space. The rms value of the beam profile is diffused following the Einstein relation which can be formulated as  $\sigma^2 \sim t$ , where  $\sigma^2$  is square of the root mean square (rms) beam size and  $t$  is the evolving time. At the Indiana University Cyclotron Facility (IUCF) Cooler ring, experiments of double rf system with phase modulation suggested which process the beam diffusion followed.

## 2 RF PHASE MODULATION EXPERIMENT

The IUCF Cooler ring is a 6-sided electron-cooled proton storage ring, which can operate from 45 to 500 MeV of kinetic energy. In the Cooler ring two rf acceleration cavities are installed. The primary cavity is a lower frequency rf system which operates from first to third harmonic, and the secondary cavity is a higher frequency system operated from sixth to ninth harmonic. For the phase modulation experiment, the proton beam was strip-injected into the Cooler ring with a kinetic energy of 45 MeV, which corresponding to a circulation frequency of about 1.03 MHz. We set the primary and the secondary rf frequencies at harmonic number  $h_1 = 1$  and  $h_2 \simeq 9$ , respectively. After injection, the proton beam was cooled by an electron beam to reduce its momentum spread. The electron cooling rate

for the Cooler ring was measured about  $3 \pm 1 \text{ s}^{-1}$ [?]. The accelerator cycle time was set as 10 s with a 3 s period before the secondary rf system and the data acquisition system turned on. The cooled beam bunch rms length was about 20 ns with a transverse momentum spread less than 0.1%. The primary rf voltage was set at about 300 V, which resulted in a synchrotron frequency of about 705 Hz while operating with the primary rf cavity alone.

The beam profile was taken by BPM sum signal passing through a low loss *elephant trunk* cable, and recorded by a fast digital scope which was set at a sampling rate of 1 ns per channel for a total of 512 or 1024 channels, while the repetitive time for the data acquisition system is about 25 to 75 particle turns. With this sampling rate we were able to investigate the detail beam profile in a single particle turn. Because the raw data for the beam profile was only a relative measurement, a background subtraction is necessary in order to obtain the real beam profile. Typically a pretrigger to start data recording was set at least 100 ns prior to the beam bunch, which gave the averaged background level in the ring. We also calculated the rms of the first 40 channels as the noise and select a signal-to-noise ratio of six as the noise cut.

### 2.1 Phase Modulation on Secondary Rf Cavity

The first experiment we did was to apply a phase modulation on the secondary rf cavity. The modulation frequency was set to cover from 100 Hz to 3600 Hz in 100 Hz steps. We also varied the modulation amplitude for several fixed frequencies. From the collected data we can investigate the following physics phenomena: the rms beam size at the initial stage and the final stage of the dilution process, the fast Fourier transform (FFT) spectra of the rms beam size and the FFT spectra of the averaged beam central position. Figure ?? shows a comparison between data and tracking simulation for the first 25 ms of the phase modulation. All the settings were identical for both top and bottom graphs. From tracking result we believe that the different physics implication between these two graphs are mainly due to the initial phase difference between the two rf systems.

For summary we compiled a graph of final rms beam size under different modulation amplitudes and modulation frequencies shown in Figure ???. Note that a sharp peak appears near 2700 Hz, about four times of the synchrotron frequency, in all modulation amplitudes except for  $A = 200^\circ$ .

## 2.2 Phase Modulation on Primary Rf Cavity

Phase modulation on the primary rf system is much more sensitive to the beam than on the secondary rf system, because the perturbation is much stronger. Thus, the modulation amplitude could only be a small angle. We also set the secondary rf frequency slightly off an integer harmonic number such that the bunch center particle density could be decreased. The effect can be seen on FFT spectra of the beam bunch centroid shown in Figure ??, where the rf harmonic ratio  $h$  for the top spectrum was 9 and for the bottom one was 8.9. The peaks near 1500 Hz found in both spectra correspond to the applied modulation frequency. However, for the  $h = 9$  case, there is another sharp peak at about 706 Hz, where was the resulting synchrotron frequency from the double rf system.

## 3 BEAM TRACKING SIMULATION

The synchrotron motion of a particle in a double-rf system with phase modulation on the secondary cavity can be written as

$$\dot{\delta} = -v_s [\sin \phi - r \sin (h\phi + \Delta\phi)] - \lambda\delta + D\xi, \quad (1)$$

$$\dot{\phi} = v_s \delta, \quad (2)$$

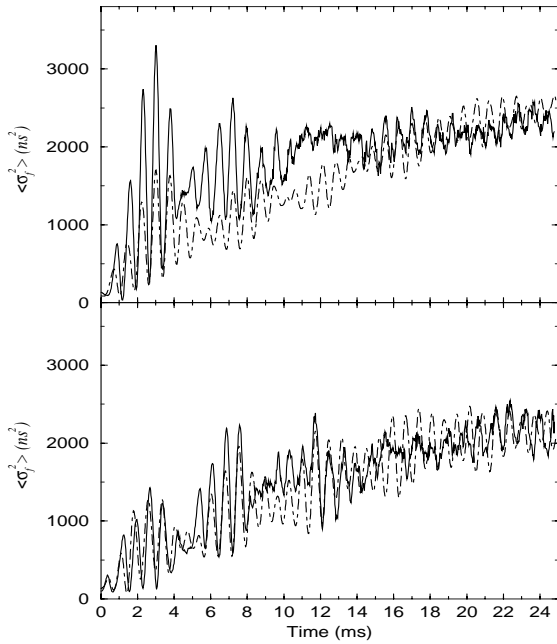


Figure 1: Examples of comparison between data (solid curves) and simulation (dashed curves) for the first 25 ms of the dilution process. The set parameters are the modulation frequency  $v_m \simeq 1200$  Hz, the modulation amplitude  $\alpha \simeq 100^\circ$  and the two rf system voltage ratio  $r \simeq 0.1$ . The parameters used in tracking are the synchrotron frequency  $f_{syn} = 723$  Hz and the initial phase difference between two cavities  $60^\circ$ . The only difference between the two figures are the initial phase for the top one is  $210^\circ$  and for the bottom one is  $140^\circ$ .

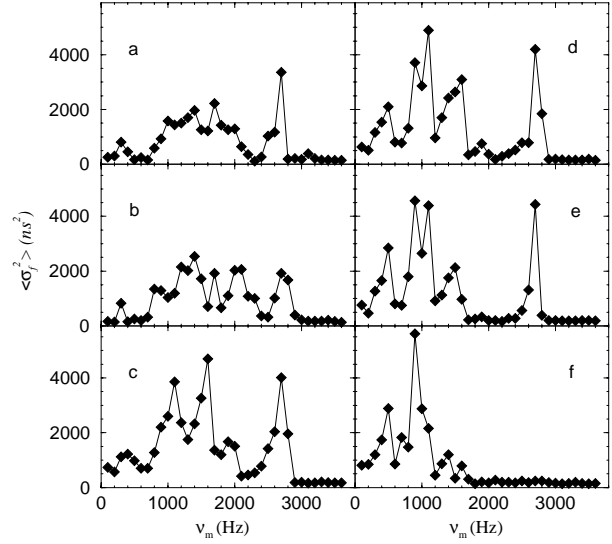


Figure 2: Averaged final rms beam size versus modulation frequency for various modulation amplitude (on the secondary rf cavity). This is done by averaging the rms beam size over the last 5 ms of the data taking ( $\langle \sigma_y^2 \rangle$ ). The alphabetic letters indicate the modulation amplitudes, where a:  $65^\circ$ , b:  $100^\circ$ , c:  $125^\circ$ , d:  $150^\circ$ , e:  $175^\circ$ , and f:  $200^\circ$ .

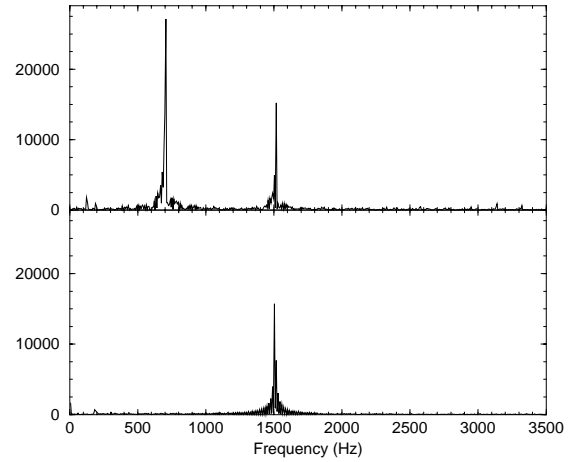


Figure 3: An example of FFT spectra for averaged center position in primary rf phase modulation. The top plot is for  $h = 9$  and the bottom plot is  $h = 8.9$ . The rf cavity voltage ratio are 0.1 for both cases.

where  $r = V_2/V_1$  is the ratio of the primary and secondary rf voltages, and  $h = h_2/h_1$  is the ratio of harmonic numbers, and  $V_1$  ( $V_2$ ) and  $h_1$  ( $h_2$ ) are the voltage gain and harmonic number for the primary (secondary) rf system. The phase of a secondary rf cavity is modulated by

$$\Delta\phi(t) = A \sin(v_m\theta + \alpha) + \Delta\phi_0,$$

where  $A$  is the modulation amplitude,  $\alpha$  is the arbitrary phase of the secondary rf phase modulation,  $v_m = f_m/f_0$

is the modulation tune, and  $\Delta\phi_0$  is a relative phase difference between two rf systems.

The evolution of the beam profile can be characterized by the rms bunch length  $\sigma^2$  defined as

$$\sigma^2 = \frac{1}{N} \sum_{i=1}^N (\phi_i - \phi_{\text{avg}})^2, \quad (3)$$

where  $N$  is the number of particles in a beam bunch and  $\phi_{\text{avg}} = \frac{1}{N} \sum_{i=1}^N \phi_i$  is the average value of  $\phi$  and where  $\phi_i$  is the  $\phi$  value of the  $i$ -th particle. A beam tracking result is shown in Figure ??.

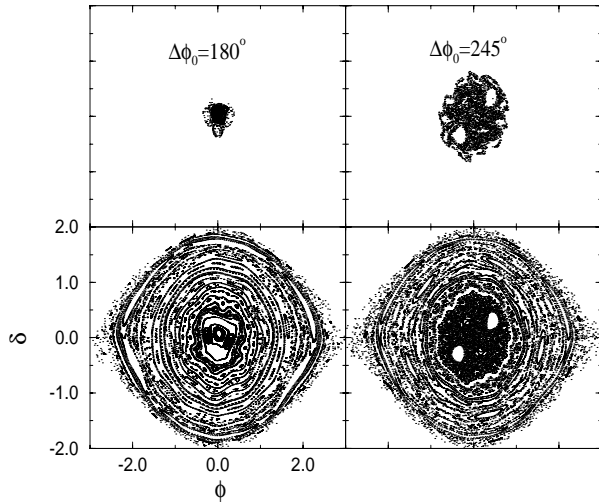


Figure 4: Poincaré surfaces of section (bottom plots) and the final beam distribution obtained from numerical simulations (top plots) for two different values of the relative phase difference  $\Delta\phi_0$ ,  $180^\circ$  and  $245^\circ$ . Beam diffusion (or dilution) occurs only when the central region of bucket becomes stochastic. The beam tracking used 4000 particles.

Because the initial beam distribution occupies only a very small area in the phase space, the final beam distribution depends on the actual chaotic region that overlaps with the initial phase space. The beam will evolve into a final distribution as shown in the upper plots of Figure ??, bounded by invariant tori[?].

## 4 CONCLUSION

Our experimental data showed that the linear growth of  $\sigma^2$  with time arises from the diffusion process in a complete chaotic region in the phase space. If the phase space possess a layer of chaotic sea with invariant tori embedded inside,  $\sigma^2$  will show characteristics of anomalous diffusion. On the other hand, if stable islands still exist in the chaotic background as shown in the lower right plot of Figure ??, the evolution of  $\sigma^2$  will be strongly oscillatory. Our experiments, with numerical simulations, have systematically verified these conditions. The understanding of the signature of the beam phase space evolution can be used to

diagnose sources of emittance dilution mechanisms in high brightness beams and space charge dominated beams.

Because of the weak damping of the electron cooling system, the rf phase modulation by a secondary rf system can provide a chaotic dynamical system, where the attractors evolve into non-intersecting attracting lines, which depends sensitively on the value of the damping decrement  $\lambda$ , and the intrinsic diffusion coefficient  $D$ . Such systems can also be detected by our beam measurement tools. Employing the sensitivity, values of  $\lambda$  and  $D$  can be independently measured.

We have experimentally measured the evolution of beam distribution as a function of rf parameters in a storage ring. The parameters which affect the dilution process are the ratio of rf voltages  $r$ , the modulation frequency  $f_m$ , the modulation amplitude  $A$ , and the relative phase  $\Delta\phi_0$ . We have found that the evolution of the bunch beam can be divided into a fast process that is related to particle diffusion along the dominate parametric resonances, and a slow process that particles diffuse inside the chaotic sea.

## 5 ACKNOWLEDGMENTS

Work supported in part by grants from the DOE-DE-FG02-92ER40747 and NSF PHY-9512832

## 6 REFERENCES

- [1] J.Y. Liu *et al.*, Particle Accelerators **49**, 221 (1995).
- [2] S.Y. Lee *et al.*, Phys. Rev. **E49**, 5717 (1994);  
J.Y. Liu *et al.*, Phys. Rev. **E50**, R3349 (1994);  
R. Averill *et al.*, Proc. of the 8th Conf. on High Energy Accelerators, edited by M. H. Blewett p.301 (CERN, Geneva, 1971);  
P. Bramham *et al.*, IEEE Trans. Nucl. Sci. **NS-24**, 1490 (1977);  
J.M. Baillod *et al.*, IEEE Trans. Nucl. Sci. **NS-30**, 3499 (1983);  
G. Gelato, L. Magnani, N. Rasmussen, K. Schindl and H. Schroenauer, Proc. IEEE Part. Acc. Conf. p.1298, March 16-19, Washington (IEEE, New York, 1987).
- [3] D. Jeon *et al.*, Phys. Rev. Lett. **80**, 2314 (1998).
- [4] M. Ellison *et al.*, Phys. Rev. Lett. **70**, 591 (1993);  
H. Huang *et al.*, Phys. Rev. **E48**, 4678 (1993);  
D. Li *et al.*, Phys. Rev. **E48**, R1638 (1993);  
D. Li *et al.*, Nucl. Inst. Methods **A 364**, 205 (1995).